AN ONLINE APPROACH FOR INTRACRANIAL PRESSURE FORECASTING BASED ON SIGNAL DECOMPOSITION AND ROBUST STATISTICS

Bin Han[1]*, Michael Muma*[2]*, Mengling Feng*[3]*, and Abdelhak M. Zoubir*[2]

[1] Institut für Industrielle Informationstechnik
Karlsruhe Institut für Technologie
Hertzstraße 16, 76187 Karlsruhe
Email: bin.han@kit.edu

[2] Signal Processing Group
Technische Universität Darmstadt
Merckstraße 25, 64283 Darmstadt, Germany
Email: {muma, zoubir}@tu-darmstadt.de

[3] Lab of Computational Physiology
Massachusetts Institute of Technology (MIT)
MIT, Cambridge, MA 02139, U.S.A.
Email: mfeng@mit.edu

ABSTRACT

Intracranial pressure (ICP) is an important physiological signal for patients with traumatic brain injuries. Accurate ICP forecasting enables active and early interventions for more effective control of ICP levels. To achieve high accuracy, most existing methods require a high sampling rate (100 Hz), which is infeasible for online medical applications. Therefore, we propose an online ICP forecasting method requiring only low rate signal sampling (0.1 Hz). Our ARIMA based forecasting method applies empirical mode decomposition (EMD) to remove non-stationarities from the ICP signal, and robust estimation to mitigate the influence of motion induced artifacts. Experimental performance assessment with simulated and clinically collected data demonstrate that the proposed method is more accurate compared to previously proposed and standard methods.

Index Terms— intracranial pressure, forecasting, non-stationarity, robustness, empirical mode decomposition

1. INTRODUCTION

A common risk for patients with traumatic brain injuries is that the primary brain damage can lead to a secondary pathophysiological damage, which usually occurs together with a significantly high or low intracranial pressure (ICP). Thus, the monitoring and prediction of ICP signals is essential. The current practice mainly relies on manual observation and judgement of nurses and clinicians, which is prone to human errors and suffers from ineffectiveness [1]. A reliable online prediction method for ICP signals is therefore sought for. The accurate prediction of an ICP signal requires dealing with a number of difficulties: First, the non-stationarity of ICP signals is too high to be cancelled by simple methods like time-differencing or short-time analysis. Second, the inevitable artifacts, which can be caused by motion of the patients or equipment errors, contaminate the signal seriously [2]. A further challenge arises from the fact that, up to now, no convincing statistical model for ICP measurements has been established.

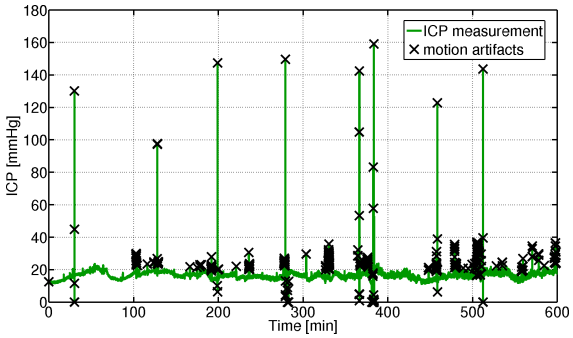

Fig. 1. Ten hour excerpt of a typical ICP measurement plotted in green. Patient motion results in inevitable measurement artifacts which are highlighted by black crosses.

Relation to Previous Work and Original Contributions

Most existing approaches, e.g. [3, 4] are based on the analysis of ICP data sampled at a high frequency (100Hz), and require simultaneous acquisition of additional medical signals. This high computational cost is inapplicable for online applications. We compare our work to [2], which also forecasts ICP signals at a low sampling frequency (0.1 Hz). Our work has its roots in signal decomposition [5, 6, 7] and robust statistics for dependent data [7, 8, 9, 10, 11].

Original contributions of our paper are: (i) A complete framework for robust online forecasting of ICP signals. (ii) A statistical model for ICP measurements. (iii) A robust artifact detection which combines decisions of a non-parametric time domain artifact detector and an ARIMA model based EMD domain detector. (iv) A computationally feasible robust ARIMA model order selection strategy. (v) An ARIMA model based robust online forecast of ICP signals in the EMD domain, which includes (vi) a robust updating stage to mitigate the effects of patchy outliers.

The paper is organized as follows. Section 2 investigates the signal characteristics and proposes a model for artifact contaminated ICP signals. Section 3 introduces our proposed method for artifact removal and signal forecasting. Section 4 provides simulation results and real data experiment results. Section 5 concludes the paper.

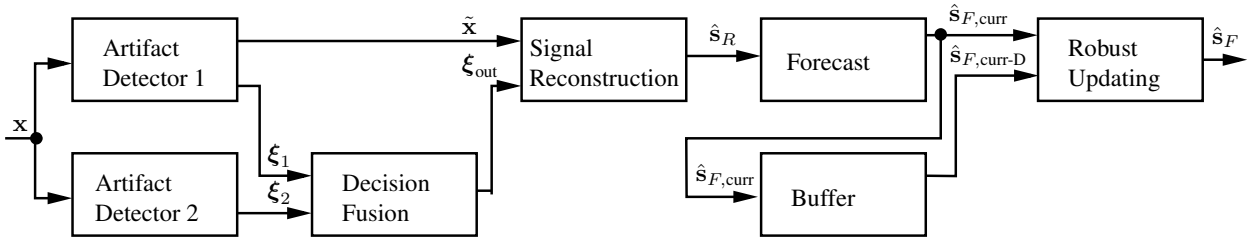

Fig. 2. Overview of the proposed robust ICP signal forecasting algorithm.

2. ANALYSIS OF ICP MEASUREMENTS AND PROPOSED MEASUREMENT MODEL

A typical ICP measurement is shown in Fig. 1. Artifacts due to patient motion and connection errors are clearly present. We therefore propose the following ICP measurement model

$$\mathbf{x} = \mathbf{s} + \boldsymbol{\nu}_1 + \boldsymbol{\nu}_2. \tag{1}$$

Here, $\mathbf{x}$ is the observed measurement, $\mathbf{s}$ is the true ICP signal, $\boldsymbol{\nu}_1$ is Gaussian white (bio-amplifier) noise and $\boldsymbol{\nu}_2$ represents the measurement artifacts. Vectors are obtained by collecting measurements at time instants $n = 0, \ldots, N-1$. Due to the nature of ICP signals, $0 < s(n) < c_s$ where c_s is a subject dependent constant.

To investigate stationarity, we applied the KPSS test [12] on a large number of hand picked artifact-free ICP measurement segments, and the results generally rejected the hypothesis of stationarity. Then, motivated by an ARIMA modelling strategy, time differencing was performed. Although the different segments can partly pass the KPSS test, the ARIMA model order estimates never converged, even for high ranges, which makes direct ARIMA modelling unsuitable for ICP signals. Extensive data analysis also showed that the stationarity length strongly varied between measurements, making a universal window choice for assuming local stationarity impossible.

The empirical mode decomposition (EMD), see [5] for details, decomposes a non-stationary series into a set of stationary components. The decomposed components are called intrinsic mode functions (IMFs). Different from the wavelet transform, the EMD requires no base wave. The non-stationary signal $\mathbf{s}$ is decomposed through EMD as follows:

$$\mathbf{s} = \sum_{i=1}^{k} \mathbf{c}_i + \mathbf{r}_k \tag{2}$$

This yields the extended IMF set $\mathscr{I}(\mathbf{s}) = \{\mathbf{c}_1, \mathbf{c}_2, \ldots, \mathbf{c}_k, \mathbf{r}_k\}^T$ of dimensions $(k+1) \times N$, where $\{\mathbf{c}_1, \mathbf{c}_2, \ldots, \mathbf{c}_k\}^T$ are IMFs and $\mathbf{r}_k$ is the residual series.

Recently, for predicting climatic data series, the authors of [6] successfully fit ARMA models to the extracted IMF components. ICP measurements, due to a higher grade of remaining non-stationarity, require ARIMA models instead of ARMA models, on each decomposed component in $\mathscr{I}(\mathbf{s})$. Data analysis with clinically collected ICP measurements showed that, for $k \geq 8$, every extended IMF can be modelled with an ARIMA model with an order vector (p, d, q), where the autoregression order $p \in [2, 20]$, the integration order $d \in [0, 2]$ and the moving average order $q \in [0, 20]$.

3. PROPOSED METHOD FOR ROBUST ICP SIGNAL FORECASTING

An overview of our method is given in Fig. 2. The following section describes the stages of our algorithm in detail.

3.1. Robust Artifact Detection and Signal Reconstruction

Assuming that a K-sample-long ICP data block $\mathbf{x}$ is read, we suggest to detect motion artifacts as outliers through the fusion of two detectors, see Fig. 2. This in general leads to better results than applying any of the individual methods separately.

Artifact Detector 1: Time Domain Median Filter

Let $\mathbf{x}$ be filtered with an i^{th}-order vector median filter with output $\tilde{\mathbf{x}}$. In practice, we empirically set $i = K/2$. Defining $\mathbf{e}_1 = \mathbf{x} - \tilde{\mathbf{x}}$, a common outlier detection rule is the 3σ rule [8]. Any measurement $x(n)$ for which $|e_1(n)| > 3\hat{\sigma}_{e_1}$, where $\hat{\sigma}_{e_1}$ is the normalized median absolute deviation (NMAD) of $\mathbf{e}_1$, is labelled as an outlier resulting in the label vector of outliers ξ_1.

Artifact Detector 2: EMD Domain ARIMA Robust Filter

As stated in [2], the motion artifacts in an ICP measurement sequence are significantly observable in the IMFs. This potentials an outlier detection in the EMD domain by using the model described in Eqs. (1) and (2) and applying the following steps:

1. Decompose $\mathbf{x}$ into its extended IMF set $\mathscr{I}(\mathbf{x})$.
2. For every row in $\mathscr{I}(\mathbf{x})$, robustly estimate its ARIMA model order (p, d, q) (see Section 3.3), extract the corresponding ARMA $(\hat{p}, \hat{q})$ process, and filter it with a

robust filter cleaner [8, 11]. Reconstruct the ARIMA process from the filtered ARMA process and subtract it from the original IMF, to obtain the vector of residuals $\boldsymbol{\epsilon}_i$ and corresponding robust scale estimate $\hat{\sigma}_i$, where i corresponds to the row index of $\mathscr{I}(\mathbf{x})$.

3. Use the overall residual vector $\mathbf{e}_2 = \sum_{i=1}^{k} \boldsymbol{\epsilon}_i$, and the overall residual scale $\hat{\sigma}_{e_2} = \sum_{i=1}^{k} \hat{\sigma}_i$ to detect artifacts analoguously as described for detector 1, resulting in the outlier label vector ξ_2.

The overall label vector of outliers ξ_{out} is obtained by the 'or' fusion of ξ_1 and ξ_2.

Signal Reconstruction

By use of ξ_{out}, $\tilde{\mathbf{x}}$ from artifact detector 1 can be used for signal reconstruction:

$$\hat{s}_R(n) = \begin{cases} x(n) & \xi_{\text{out}}(n) = 0 \\ \tilde{x}(n) & \xi_{\text{out}}(n) = 1 \end{cases}$$

Collecting the time instants into a vector yields $\hat{\mathbf{s}}_R$, the artifact cleaned ICP signal, see Fig. 2.

3.2. Proposed Forecasting Approach

Assuming perfect artifact removal, classical forecasting methods, e.g. the Kalman filter can be applied. In case of imperfect reconstruction, we suggest either to use a robust Kalman filter [8, 13], or to:

1. Decompose $\hat{\mathbf{s}}_R$ with EMD into its extended IMF set $\mathscr{I}(\hat{\mathbf{s}}_R)$.

2. For every component in $\mathscr{I}(\hat{\mathbf{s}}_R)$, robustly estimate its ARIMA model, to obtain a robust ARIMA forecast, e.g. with the median of ratios estimator [9].

3. Sum all forecast components up to obtain the overall forecast signal $\hat{\mathbf{s}}_{F,\text{curr}}$.

Robust Updating for Patchy Outlier Mitigation

For ICP measurements, the common concept of i.i.d. outliers is not applicable. In fact, artifacts create bursts of outliers, so called patchy outliers [8, 11], which appear due to non-uniform patient motion. Clearly, the forecasts based on some data blocks will be much worse than others, even when using robust methods. To deal with this, we suggest to save the current forecast in a buffer (see Fig. 2), therewith allowing for forecasts $\hat{\mathbf{s}}_{F,\text{curr}}$ and $\hat{\mathbf{s}}_{F,\text{curr-D}}$, which overlap on an interval of length D. We next assess the forecasting quality in the spirit of John W. Tukey's comment [14] that robust and non-robust methods significantly differ, only when outliers are present. Therefore, we compute (non-robust) sample standard deviations of $\hat{\mathbf{s}}_{F,\text{curr}}$ and $\hat{\mathbf{s}}_{F,\text{curr-D}}$ on D and compare them to a robustly estimated scale of measurements $x(n)$ for which $\xi_{\text{out}}(n) = 0$. The final forecast $\hat{\mathbf{s}}_F$ (see Fig. 2) is then obtained by the prediction whose standard deviation is closer to robust scale estimate.

3.3. Fast Robust ARIMA Model Order Selection

In presence of outliers, classical model order selection criteria break down and robust methods (see e.g. [15, 16] and references therein) have been proposed. For artifact detector 2 and for the forecast stage (see Figure 2), the ARIMA model order (p, d, q) must be estimated for every extended IMF component. Approximate model order selection based on the decay of the auto-covariance function (ACF) and the partial auto-covariance function (PACF) [17] is widely used, because of its low computational complexity. Here, we adapt this method by robustifying the estimators of the ACF and the PACF due to the artifacts. We suggest to use the robust and computationally simple median of ratios estimator for the ACF whose robustness properties are discussed in [9]. The PACF then can be estimated with the help of the estimated ACF through a Levinson-Durbin recursion.

4. RESULTS

In this section, the effectiveness of the proposed method is experimentally evaluated through both simulated and real ICP signals.

4.1. Simulations and Performance Evaluation

Due to the absence of a ground truth synthetic statistical model for ICP signals, it is impossible to simulate an ICP signal perfectly. Here, we adapt two different motion models, i.e. the random walk model and the velocity sensor model to approximate the stable and unstable ICP signals, and to account for inaccuracy of our suggested ICP signal model. Patchy artifacts are generated by expanding isolated artificial pulses with MA filters, as described in [7]. Simulation parameters are as follows. Sampling frequency $f_s = 0.1$ Hz; sample length $N = 2500$; random walk noise deviation $\sigma_{\text{rw}} = 0.1$; initial signal value $s(0) = 25$mmHg; $\nu_1(n) \sim \mathcal{N}(0, 1)$; for $\nu_2(n)$: $\text{prob}(\nu_2(n) \neq 0) = 0.01$ and maximum patch duration and amplitude are modelled by uniform distributions with empirically set parameters; forecast horizon = training length = 360; $D = 90$.

To evaluate the performance, the following three metrics are defined: (i) The outlier detection accuracy (ODA):

$$\text{ODA} = 1 - 0.05 p_{\text{FA}} - 0.95 p_{\text{MD}},$$

where p_{FA} is the false alarm rate and p_{MD} is the missed detection rate. (ii) The mean signal reconstruction error (MSRE):

$$\text{MSRE} = \frac{1}{N} \sum_{n=0}^{N-1} \left| \frac{\hat{s}_R(n) - s(n)}{s(n)} \right|,$$

and (iii) the 10-percent gross prediction error rate (GPER):

$$\text{GPER} = \frac{1}{N}\sharp\{n \mid \left|\frac{\hat{s}_F(n) - s(n)}{s(n)}\right| > 0.1\},$$

where $\sharp\{\cdot\}$ denotes the number of elements in a set. Average results based on 100 Monte Carlo runs, are shown in Tables 4.1 and 4.1. Here, NN stands for the neural networks based method described in [2], KF ARIMA represents our method using a Kalman filter forecasting (assuming perfect artifact removal, see Section 3.2), and ROB ARIMA denotes our method using robust ARIMA forecasting. Both our methods use the suggested robust updating, which in general lowered the GPER (best GPER without: ROB ARIMA 9.20% for random walk, ROB ARIMA 8.54% for velocity sensor).

	ODA	MSRE	GPER
NN	99.61%	3.34%	100%
KF ARIMA	99.58%	3.13%	11.35%
ROB ARIMA	99.58%	3.13%	3.53%

Table 1. Averaged evaluation metrics based on simulated data using the random walk model.

	ODA	MSRE	GPER
NN	99.67%	3.43%	100%
KF ARIMA	99.62%	3.22%	13.28%
ROB ARIMA	99.62%	3.22%	4.19%

Table 2. Averaged evaluation metrics based on simulated data using the velocity sensor model with additive outliers.

4.2. Real Data Experiment Results

To validate real data suitability, online forecasting is applied to clinically collected ICP measurements. Due to the lack of a ground truth for the ICP signal, it is impossible to compute the evaluation metrics. However, a qualitative evaluation can be made through visual inspection. Examples are shown in Fig. 3.

5. CONCLUSIONS

An online approach for robust ICP signal forecasting was presented. Simulations results show good performance, i.e. a GPER below 5 % in situations where the approach by [2] fails. Visual inspection of clinically measured ICP signals indicates stable performance, even in seriously contaminated data sets.

Acknowledgements

We would like to thank clinicians and nurses from National Neuroscience Institute, Singapore, for their efforts in data collection and clinical advices. This work was partially supported by the SERC grant 092-148-0067 of Agency for Science, Technology and Research, Singapore.

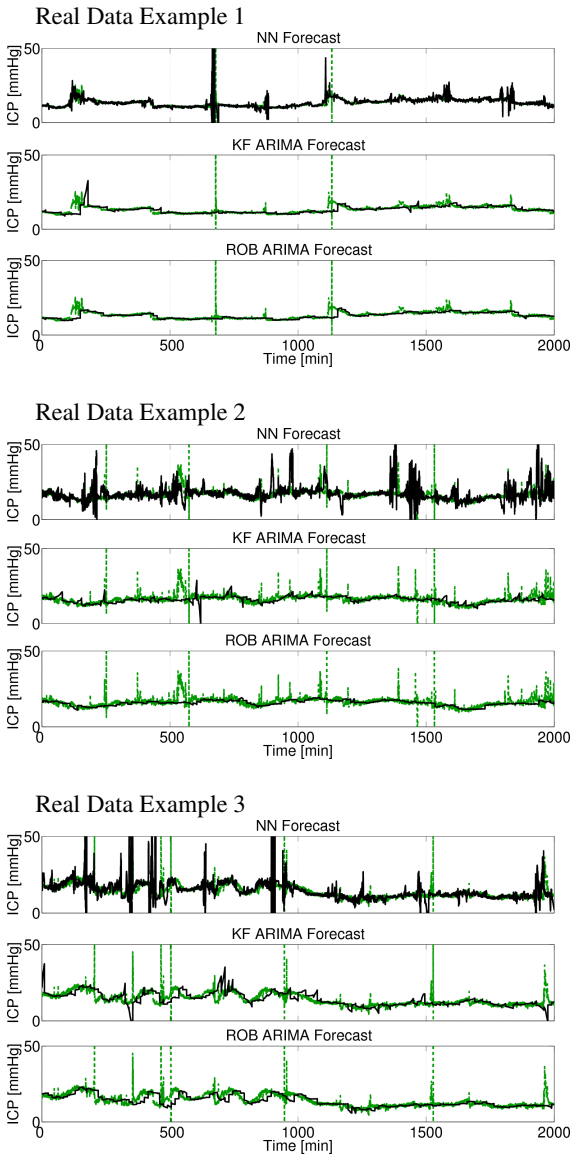

Fig. 3. Online forecast results for three different subjects for a time-span of 33 hours and 20 minutes. The raw measurements are plotted in green, while the three online forecasts are depicted in black. Real Data Example 1 is a measurement with a small amount of artifacts, while Real Data Examples 2 and 3 are highly contaminated. The third example has been chosen, to illustrate forecast performance for quickly varying ICP levels. In all cases, subjective visual inspection suggests that the proposed methods render more stable and accurate forecasts compared to the existing method based on neural networks. The robust ARIMA forecast provides best results and resists outliers caused by motion artifacts even in these difficult situations.

6. REFERENCES

[1] M. Feng and Z. Zhang. "ISYNCC: An intelligent system for patient monitoring and clinical decision support in neuro-critical-care." In *Proc. IEEE Int. Conf. Eng. in Medicine and Biology Society (EMBC 2011)*, pp. 6426–6429.

[2] M. Feng, L.Y. Loy, F. Zhang, and C. Guan. "Artifact removal for intracranial pressure monitoring signals: A robust solution with signal decomposition." In *Proc. IEEE Int. Conf. Eng. in Medicine and Biology Society (EMBC 2011)*, pp. 797–801.

[3] X. Hu, P. Xu, S. Asgari, P. Vespa, and M. Bergsneider. "Forecasting ICP elevation based on prescient changes of intracranial pressure waveform morphology." *IEEE Trans. Biomed. Eng.*, vol. 57, no. 5, pp. 1070–1078, May 2010.

[4] X. Hu, P. Xu, F. Scalzo, P. Vespa, and M. Bergsneider. "Morphological clustering and analysis of continuous intracranial pressure." *IEEE Trans. Biomed. Eng.*, vol. 56, no. 3, pp. 696–705, March 2009.

[5] Z. Shen, S.R. Long, M.C. Wu, H.H. Shih, Q. Zheng, N.C. Yen, C.C. Tung, and H.H. Liu. "The empirical mode decomposition and Hilbert spectrum for nonlinear and nonstationary time series analysis." *Proc. Roy. Soc. London. Series A: Mat.*, vol. 454, no. 1971, pp. 903–995, March 1998.

[6] P. Yang, G. Wang, and J. Bian. "The prediction of non-stationary climate series based on empirical mode decomposition." *Adv. Atmos. Sci.*, vol. 27, no. 4, pp. 845–854, July 2010.

[7] F. Strasser, M. Muma, and A.M. Zoubir. "Motion artifact removal in ECG signals using multi-resolution thresholding." in *Proc. 20th European Signal Processing Conference (EUSIPCO 2012)*, pp. 899–903.

[8] A.M. Zoubir, V. Koivunen, Y. Chakhchoukh, and M. Muma. "Robust estimation in signal processing: a tutorial-style treatment of fundamental concepts." *IEEE Signal Proc. Mag.*, vol. 4, no. 29, pp. 61–80, 2012.

[9] Y. Chakhchoukh. "A new robust estimation method for ARMA models." *IEEE Trans. Signal Processing*, vol. 58, no. 7, pp. 3512 –3522, July 2010.

[10] R.D. Martin and D.J. Thomson. "Robust-resistant spectrum estimation." *Proc. IEEE*, vol 70, no. 9, pp. 1097–1115, 1982.

[11] R.A. Maronna, R.D. Martin, and V.J. Yohai. *Robust statistics: Theory and methods*. Wiley Series in Probability and Statistics, 2006.

[12] D. Kwiatkowski, P.C.B. Phillips, P. Schmidt, and Y. Shin. "Testing the null hypothesis of stationarity against the alternative of a unit root." *J. Econometrics*, vol. 54, no. 1-3, pp. 159–178, 1992.

[13] S. Farahmand, G.B. Giannakis, and D. Angelosante. "Doubly Robust Smoothing of Dynamical Processes via Outlier Sparsity Constraints." *IEEE Trans. Signal Processing*, vol. 59, no. 10, pp. 4529–4543, Oct 2011.

[14] P.J. Huber. "John W. Tukey's contributions to robust statistics." *Ann. Statist.*, vol. 30, no. 6, pp. 1640–1648, December 2002.

[15] M. Muma and A.M. Zoubir. "Robust Model Selection for Corneal Height Data Based on Tau Estimation." In *Proc. IEEE Int. Conf. on Acoustics, Speech and Signal Processing (ICASSP 2011)*, pp. 4096 - 4099.

[16] M. Muma, Y. Cheng, F. Roemer, M. Haardt, and A. M. Zoubir. "Robust source number enumeration for R-dimensional arrays in case of brief sensor failures." In *Proc. IEEE Int. Conf. on Acoustics, Speech and Signal Processing (ICASSP 2012)*, pp. 3709–3712.

[17] G.E.P. Box, G.M. Jenkins, and G.C. Reinsel. *Time Series Analysis: Forecasting and Control.* Wiley Series in Probability and Statistics, Fourth Edition, 2008.